Title

Multi-omic analyses of exogenous nutrient bag decomposition by the black morel Morchella importuna reveal sustained carbon acquisition and transferring

Journal

Environmental Microbiology, 21(10)

ISSN

1462-2912

Authors

Tan, Hao
Kohler, Annegret
Miao, Renyun
et al.

Publication Date

2019-10-01

DOI

10.1111/1462-2920.14741

Peer reviewed

Multi-omic analyses of exogenous nutrient bag decomposition by the black morel *Morchella importuna* reveal sustained carbon acquisition and transferring

Hao Tan,[1,2]* Annegret Kohler,[3] Renyun Miao,[1,2] Tianhai Liu,[1,2] Qiang Zhang,[1,2] Bo Zhang,[1,2]
Lin Jiang,[1,2] Yong Wang,[1,2] Liyuan Xie,[1,2] Jie Tang,[1,2] Xiaolin Li,[1,2] Lixu Liu,[1,2] Igor V. Grigoriev,[4,5]
Chris Daum,[4,5] Kurt LaButti,[4,5] Anna Lipzen,[4,5] Alan Kuo,[4,5] Emmanuelle Morin,[3] Elodie Drula,[6,7,8] Bernard Henrissat,[6,7,8] Bo Wang,[1,2]
Zhongqian Huang,[1,2] Bingcheng Gan,[1,2] Weihong Peng[1,2] and Francis M. Martin[3]*

[1]*National-Local Joint Engineering Laboratory of Breeding and Cultivation of Edible and Medicinal Fungi, Mushroom Research Center, Soil and Fertilizer Institute, Sichuan Academy of Agricultural Sciences, Chengdu, China.*

[2]*Scientific Observing and Experimental Station of Agro- Microbial Resource and Utilization in Southwest China, Ministry of Agriculture, Chengdu, China.*

[3]*Université de Lorraine, Institut National de la Recherche Agronomique, UMR Interactions Arbres/Microorganismes, Centre INRA-GrandEst, Champenoux, 54280, France.*

[4]*US Department of Energy Joint Genome Institute, Walnut Creek, CA, USA.*

[5]*Department of Plant and Microbial Biology, University of California Berkeley, Berkeley, CA, USA.*

[6]*Architecture et Fonction des Macromolécules Biologiques, CNRS, Aix-Marseille University, Marseille, F-13288, France.*

[7]*Institut National de la Recherche Agronomique, USC1408 Architecture et Fonction des Macromolécules Biologiques, Marseille, F-13288, France.*

[8]*Department of Biological Sciences, King Abdulaziz University, Jeddah, 21589, Saudi Arabia.*

Summary

The black morel (*Morchella importuna* Kuo, O'Donnell and Volk) was once an uncultivable wild mushroom,

until the development of exogenous nutrient bag (ENB), making its agricultural production quite feasible and stable. To date, how the nutritional acquisition of the morel mycelium is fulfilled to trigger its fruiting remains unknown. To investigate the mechanisms involved in ENB decomposition, the genome of a culti- vable morel strain (*M. importuna* SCYDJ1-A1) was sequenced and the genes coding for the decay appara- tus were identified. Expression of the encoded carbohydrate-active enzymes (CAZymes) was then ana- lyzed by metatranscriptomics and metaproteomics in combination with biochemical assays. The results show that a diverse set of hydrolytic and redox CAZymes secreted by the morel mycelium is the main force driv- ing the substrate decomposition. Plant polysaccharides such as starch and cellulose present in ENB substrate (wheat grains plus rice husks) were rapidly degraded, whereas triglycerides were accumulated initially and consumed later. ENB decomposition led to a rapid increase in the organic carbon content in the surface soil of the mushroom bed, which was thereafter con- sumed during morel fruiting. In contrast to the high car- bon consumption, no significant acquisition of nitrogen was observed. Our findings contribute to an increas- ingly detailed portrait of molecular features triggering morel fruiting.

Introduction

Species in the fungal genus *Morchella*, commonly known as morels, are important gourmet mushrooms. Morels possess diverse ecological types including saprotrophic, pyrophilic and ectomycorrhizal, and the boundary of eco- logical types can be vague (Pilz *et al*., 2004). Commercial demand for morel in world market is constantly growing, despite their high prize (Tietel and Masaphy, 2018). Due to limited production of wild morels, attempts to cultivate morels artificially started over 130 years ago (Roze, 1882). Ascocarps (fruiting bodies) were once produced in walk-in growth chambers (Ower *et al*., 1989), but further development of this method ceased, as repeating Ower's success by others has proven difficult (Masaphy, 2010). Although several kinds of morel cultivating techniques

emerged in the last two decades (Liu *et al*., 2018), morel cultivation industry was boosted only after the breeding of several black morel varieties with improved fruiting yield and stability (Peng *et al*., 2016; Liu *et al*., 2018), and more importantly, the development and widespread application of an appropriate organic substrate contained in the so-called exogenous nutrient bag (ENB), a special type of culture substrate enriched in plant polysaccharides. Thanks to the ENB technique, cultivation of black morel expanded rapidly in China from 200 ha in 2011 to over 1200 ha in 2015 (Liu *et al*., 2016), which generated the exportation of dried fruiting bodies from 180 to 900 tons between 2011 and 2015 (Du *et al*., 2015). Despite its widespread application, the decomposition mechanisms taking place in ENB remain to be determined.

Use of ENB is the key technique that allowed large- scale ascocarp formation from the *Morchella elata* clade (O'Donnell *et al*., 2011). It was initially developed in 2000 as a prototype (Tan, 2016), improved later and evolved to the present form. The most prevalent ENB formulation today is a plastic bag filled with wheat grains plus rice husks, and then autoclaved. After piercing or cutting its bottom casing to allow colonization by morel mycelium from the soil, ENBs are placed on the surface of soil inoc- ulated with black morel, the so-called mushroom bed (Fig. 1A and B). The mushroom bed is an outdoor soil ecosystem containing natural microbial inhabitants, rather than a quasi-sterile environment. The cultivation method for black morel is unique, very different from the cultivation of usual edible mushrooms such as *Pleurotus ostreatus*, *Lentinus edodes*, *Agaricus bisporus* (Chang and Hayes, 2013) and *Coprinus comatus* (Stojkovi‚c *et al*., 2013). For unknown reasons, ENB is required for high-yield and sta- ble fruiting of black morel. It is believed that ENB provides key organic nutrients, (C) source for morel mycelium and is considered as a spe- cial type of mushroom culture substrate (Fig. 1C).

Wild morels are able to produce fruiting bodies on vari- ous types of substrates, such as post-fire forest soils (Larson *et al*., 2016), plant debris as well as living roots (Pilz *et al*., 2004; 2007). In post-fire soils, wild morels are unlikely to consume recent plant litter as primary C and nitrogen (N) sources (Hobbie *et al*., 2016). Compared with the contingent fruiting in the wild, ENB provides a highly reproducible system which allows the black morel to complete its life cycle in an artificial environment. It is particularly helpful for studying physiological and bio- chemical processes driving the fruiting of soil saprotrophic mushrooms.

To investigate the mechanisms involved in ENB decom- position, genome of *Morchella importuna* was sequenced and genes coding for the decay apparatus were identified. Expression of the encoded carbohydrate-active enzymes (CAZymes) was then analyzed by metatranscriptomics and metaproteomics in combination with bioassays.

Results

Genome features

The Illumina-sequenced haploid genome of *M*. *importuna* SCYDJ1-A1, a cultivable strain from China, resulted in a 48.80 Mbp assembly, with an average read-depth cover- age of 84× in 338 scaffolds (scaffold N50 = 27; Supporting Information Table S1). By using the JGI Annotation Pipe- line (Grigoriev *et al*., 2014), we identified 11 971 genes (Supporting Information Table S2). The assembly size of the haploid genome of an European wild strain, *M*. *importuna* CCBAS932, was 48.21 Mbp (Supporting Infor- mation Table S1), with a similar number of encoded genes

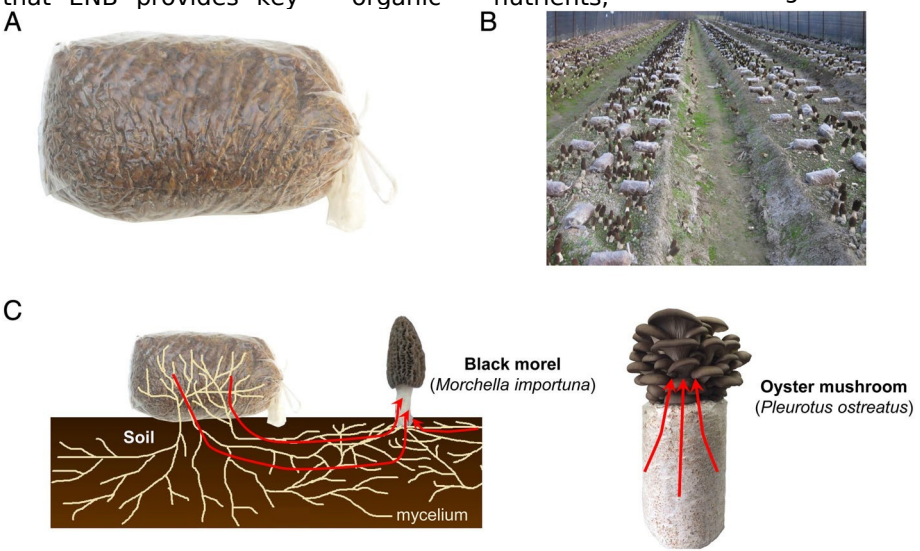

Fig. 1. A. ENB for morel cultivation. B. Large-scale morel cultivation showing ENB laying on the mush- room bed in a greenhouse. C. The method of cultivation of black morels using ENB differs from the cultivation methods used for other commercial mushrooms, such as the oyster mush- room (*P*. *ostreatus*), where fruiting bod- ies are produced directly from the

bag containing a lignocellulosic substrate. Red arrow means flow of organic nutrients. [Color figure can be viewed at wileyonlinelibrary.com]

(11 600; Murat *et al*., 2018). The completeness of genome assemblies of the two strains are similar (Supporting Infor- mation Table S1). Pairwise synteny of scaffolds between the two strains was estimated by the vista synteny tool (Martin *et al*., 2004) available at JGI genome portals of *Morchella*. Almost every scaffold from the genome of strain SCYDJ1-A1 had a highly syntenic scaffold hit from the strain CCBAS932 (Supporting Information Fig. S1). The two strains share 9783 common genes as determined by BlastP Best Reciprocal Hit analysis (Supporting Infor- mation Table S3). Strains SCYDJ1-A1 and CCBAS932 possessed 9891 and 9873 core-genes, respectively, whereas strain-specific genes were 2080 and 1727 (Supporting Information Table S2). Most strain-specific proteins are small proteins with unknown functions or no PFAM domains. The results indicate that the two *M*. *importuna* genomes are highly syntenic, whereas their gene repertoires are substantially divergent. Genome sequences, gene models and annotations of the two *M*. *importuna* strains are publicly available from the JGI MycoCosm database (Grigoriev *et al*., 2014). Their func- tional portraits (GO, KEGG and KOG) are very similar (available online from their JGI genome portals). The geno- mic information indicates that *M*. *importuna* SCYDJ1-A1 has the capacity to secrete a large repertoire of CAZymes, including glycoside hydrolases (GH), glycosyl transferases (GT), carbohydrate esterases (CE), polysaccharide lyases (PL) and several auxiliary activity enzymes (AA). Most of the CAZymes are plant cell wall degrading enzymes predicted to possess decomposition capabilities for plant polysaccharides such as cellulose, hemicellulose and pec- tins. Together, the results indicate the potential of *M*. *importuna* to degrade a large set of substrates found in decaying plant debris. To obtain experimental evidence for the hydrolytic capabilities of *M*. *importuna* SCYDJ1-A1 against plant polysaccharides, profiling of transcripts and proteins (see below) was performed on ENB extracts after 15, 45 and 75 days of growth.

ENB affects morel yield

M. *importuna* SCYDJ1-A1 was cultivated in a pre-homogenized soil (Supporting Information Table S4), which was used as the mushroom bed in this study. During the entire cultivation course, the temperatures inside ENB fluctuated between 6^0C and 13^0C (Supporting Information Fig. S2). ENB weight showed no significant change over the first 15 days (days 0–15) after contact with the mush- room bed [p-value = 0.727, by one-way analysis of vari- ance (ANOVA)] but shrank progressively from day 15 to day 75 (day 45 < day 15, p-value = 8.50×10^{-6}; day 75 < day 45, p-value = 9.15×10^{-5}, by one-way ANOVA; Fig. 2A). About 34% of the ENB dry weight was consumed during days 15–45, with an additional 23% during days

45–75, indicating a sustained consumption of organic nutri- ents. Indeed, total C content per ENB decreased at a slow rate during days 0–15 (p-value = 0.037, by one- way ANOVA), then at a higher rate during days 15–45 (p-value = 6.29×10^{-4}, by one-way ANOVA), before reaching a plateau during days 45–75 (p-value = 0.110, by one-way ANOVA) (Fig. 3A; Supporting Information Table S5), suggesting that ENB substrate was con- sumed majorly in the middle stage. In response to ENB decomposition, total organic C in the surface soil (Fig. 2B) was increased significantly during days 15–45 (p-value = 3.41×10^{-8}, by one-way ANOVA) and days 45–75 (p-value = 9.19×10^{-3}, by one-way ANOVA). After that, morel fruiting consumed a lot of the accumu- lated organic C, by comparing day 75 with the comple- tion of fruiting body harvest (p-value = 1.09×10^{-7}, by one-way ANOVA). After harvest, organic C in the sur- face soil was still higher than the initial level before morel sowing (6.04 ± 0.05 g kg^{-1}) (p-value = 3.91×10^{-4}, by one-way ANOVA; Fig. 2B).

Total N in ENB increased significantly during days 0–15 (p-value = 0.023, by one-way ANOVA; Fig. 3A; Supporting Information Table S5), likely a result of ENB colonization by the morel mycelium and other microbes. In response, a temporary fall of inorganic ammonium N in the surface soil took place during days 0–15 (p-values between 4.06×10^{-4} and 5.68×10^{-4}, by one-way ANOVA). After 15 days, total N content in ENB decreased slowly until returned to its initial level (day 75 similar to day 0, p-value = 0.645, by one-way ANOVA). It suggests that N was not substantially exported from ENB to the surface soil.

Total C consumption in ENB was much higher than total N (Fig. 3A) (p-value = 1.41×10^{-6}, by t test), which is supported by strikingly high activities of amylases and lipases detected in ENB (Fig. 3B). The imbalance between C and N consumptions resulted in a continuous decrease in C:N ratio, from 36.9 to 19.3 (Fig. 3A). Total P and total K were both consumed continuously from day 0 to day 75 (p-value = 8.31×10^{-5} and 1.66×10^{-7}, respectively, by one-way ANOVA).

The duration of ENB contact with the mushroom bed influenced fruiting body yield profoundly (Fig. 2A). Without ENB, no fruiting took place, confirming that the nutrients released by decaying ENB substrate are required for fruiting. Removing ENB at day 15 or day 45 stopped the increase in soil organic C (day 45 similar to day 15, p-value = 0.999; day 75 < day 45, p-value = 0.001, by one-way ANOVA) and also lowered the fruiting body yield significantly (p-value = 3.73×10^{-10} and 4.46×10^{-6}, respectively, by one-way ANOVA). It indicates that the consumed organic compounds from ENB were transferred to the underlying soil, while future experiments with nets to avoid mycelium colonization would be helpful to confirm

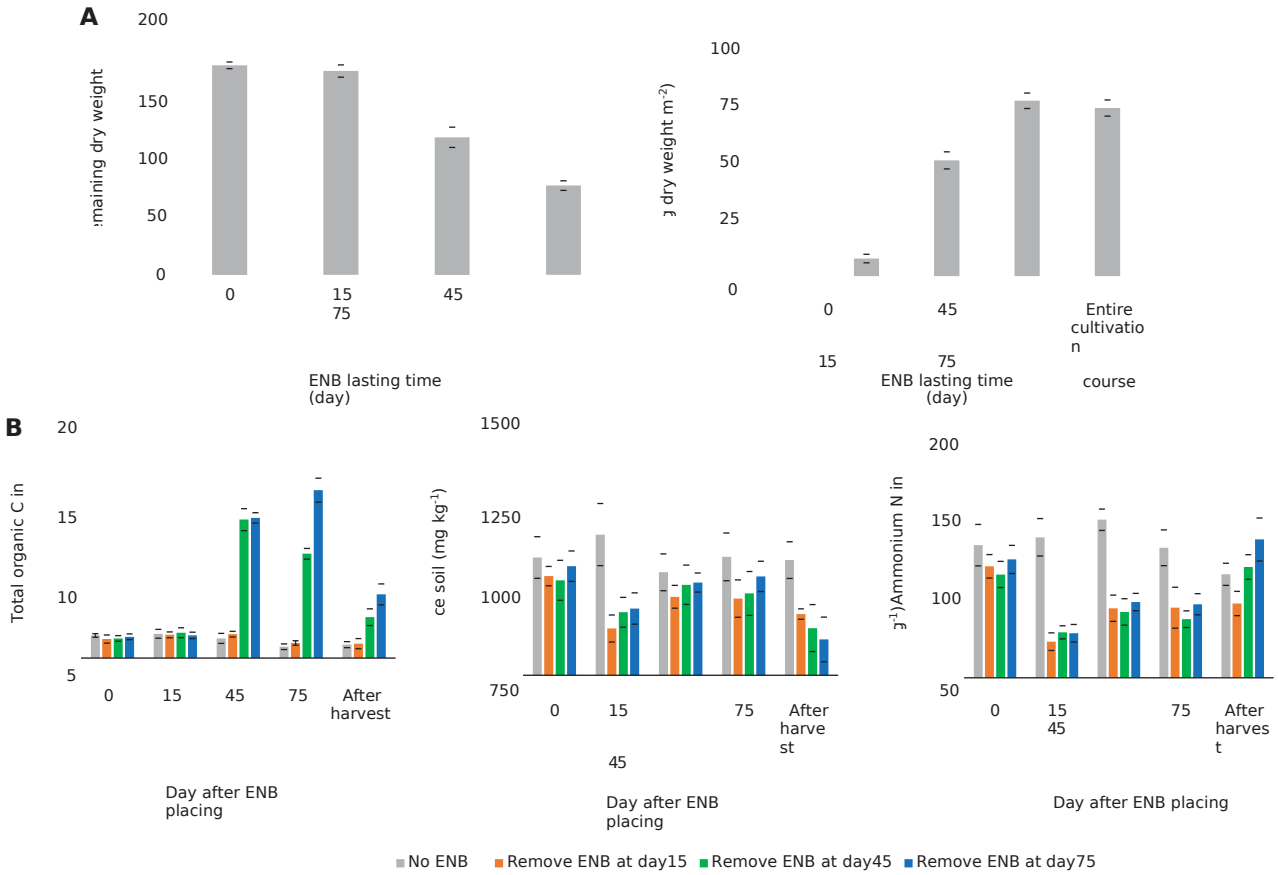

Fig. 2. A. The ENB substrate was consumed while the yield of morel fruiting body increased simultaneously. B. Time-course changes in total organic C, total N and ammonium N in the surface soil. The coloured columns show mean of three biological replicates, with standard deviation bars. Significant difference in multi-group comparison of an item at the three time-points was judged by one-way ANOVA. Significant difference in pairwise comparison of two items at the same time-point, or during the same period, was judged by *t* test. A full list of all *p*-values is provided in Supporting Information Table S8.

the translocation through mycelial networks. Keeping ENB until all fruiting bodies were harvested, the yield showed no significant difference with removing ENB at day 75 (*p*- value = 0.660, by one-way ANOVA; Fig. 2A). It means that keeping ENB on the mushroom bed for at least 75 days is essential to get as high yield as possible. Moreover, the duration of ENB contact with the mushroom bed also influenced the contents of total N, total proteins and free amino acids in morel fruiting bodies (Supporting Informa- tion Fig. S3).

Carbohydrate decomposition

A diverse array of CAZymes encoded by *M. importuna* were identified in decaying ENB and their expression strikingly varied along the time-course of decomposition (Fig. 4). Consequently, carbohydrates as the major frac- tion in ENB were degraded and consumed rapidly. About 70% of total carbohydrates were lost in 75 days. Amylo- pectin, amylose and cellulose, consumed in large quan- tity (Fig. 3A), were the most prominent C source for metabolism. Over 90% of amylose was metabolized dur- ing days 0–75, whereas amylopectin was metabolized by 72%. The consumed proportion of amylose was higher than amylopectin (*p*-value = 8.73×10^{-5}, by *t* test), although the content of amylopectin in ENB was nearly

twice higher than amylose. The high degrading rates of amylopectin and amylose are supported by the high γ-amylase activity (Fig. 3B). A GH15 protein identified in ENB (Fig. 4) seemed responsible for the γ-amylase activ- ity. Its upregulated expression [fold-change = 5.79 during days 15–45, p-value = 5.56×10^{-4}, by t test with false discovery rate (FDR) correction for multiple testing] was similar with the growing trend of γ-amylase activity observed during days 15–75 (day 45 > day 15, p-value = 0.002; day 75 > day 45, p-value = 1.84×10^{-5}, by FDR-corrected t test; Fig. 3B). In comparison, the other amylases involved in starch hydrolysis showed much lower activities (Fig. 3B). The GH13 proteins were annotated as starch-hydrolysis-related enzymes, includ- ing two α-amylases, an α-glucosidase, a branching enzyme and a debranching enzyme (Fig. 4). Like the γ-amylase, the upregulated expression of GH13_1 and GH13_m42 proteins (GH13_1: fold-change = 5.42 during days 15–45, p-value = 0.001; GH13_m42: fold- change = 5.06 during days 15–45 and 2.70 during days 45–75, p-value = 5.35×10^{-4} and 1.16×10^{-4}, respec- tively, by FDR-corrected t test) supports the observed increase in α-amylase activity (day 45 > day 15, p- value = 2.30×10^{-3}; day 75 > day 45, p-value = 0.004, by FDR-corrected t test; Fig. 3B). As *M*. *importuna* genome lacks β-amylase gene (GH14), the observed

A

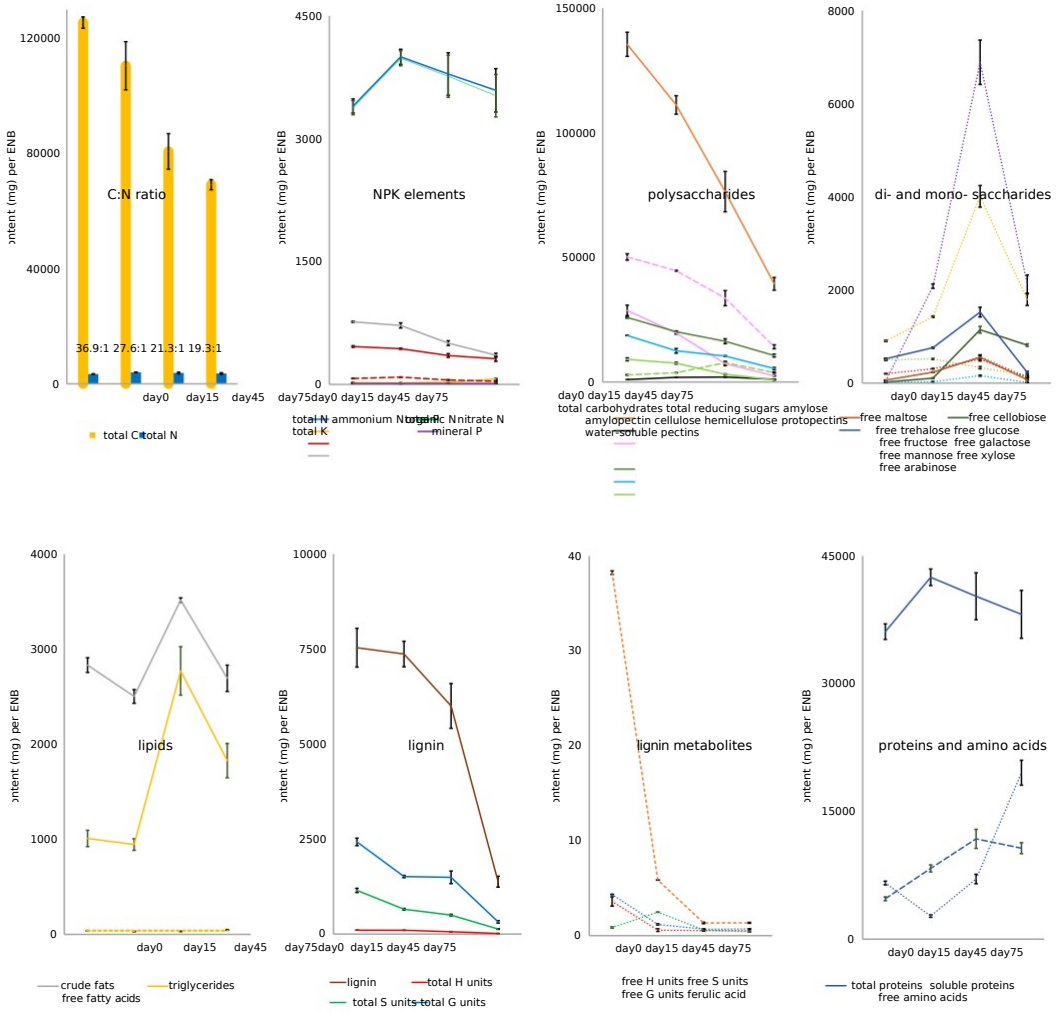
C:N ratio
36.9:1 27.6:1 21.3:1 19.3:1
total C total N
NPK elements
total N ammonium N nitrate N
total K
mineral P
polysaccharides
total carbohydrates total reducing sugars amylose
amylopectin cellulose hemicellulose protopectins
water-soluble pectins
di- and mono- saccharides
free maltose
free cellobiose
free trehalose free glucose
free fructose free galactose
free mannose free xylose
free arabinose
lipids
crude fats
free fatty acids
triglycerides
lignin
lignin
total H units
total S units
total G units
lignin metabolites
free H units free S units
free G units ferulic acid
proteins and amino acids
total proteins soluble proteins
free amino acids
day0 day15 day45 day75

B

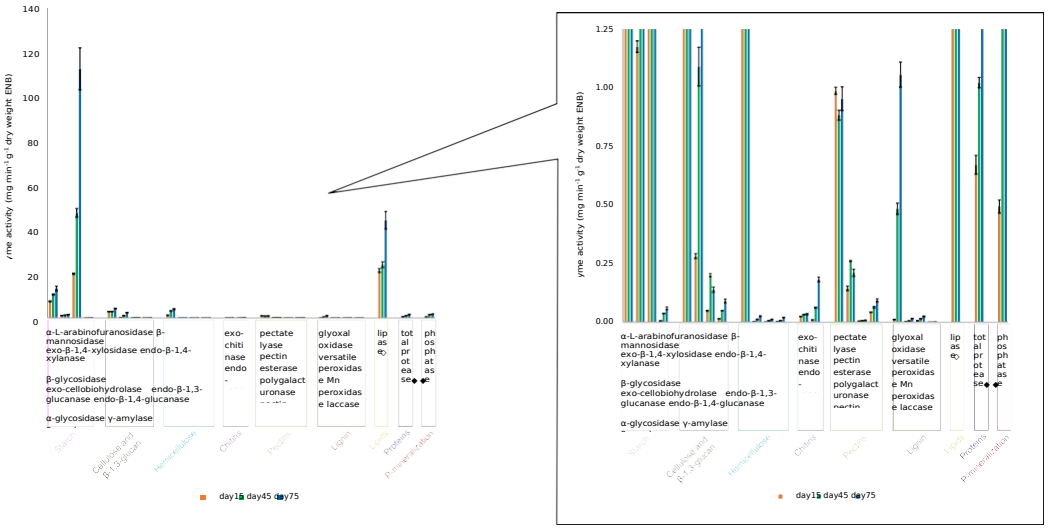
α-L-arabinofuranosidase β-mannosidase
exo-β-1,4-xylosidase endo-β-1,4-xylanase
β-glycosidase
exo-cellobiohydrolase endo-β-1,3-glucanase endo-β-1,4-glucanase
α-glycosidase γ-amylase
exo-chitinase endo-
pectate lyase pectin esterase polygalacturonase
glyoxal oxidase versatile peroxidase Mn peroxidase laccase
lipase
total protease
phosphatase
Starch
Cellulose and β-1,3-glucan
Hemicellulose
Chitins
Pectin
Lignin
Lipids
Proteins
P-mineralization
day15 day45 day75

Fig. 3. Legend on next page.

β-amylase activity was likely produced by other microbes colonizing ENB.

The activity of endo-cellulase (endo-β-1,4-glucanase) increased slightly during days 15–45 (p-value = 0.612, by one-way ANOVA) and significantly during days 45–75 (p- value = 1.53×10^{-5}, by one-way ANOVA). The activities of exo-cellulase (exo-β-1,4-glucanase) and β-glycosidase were much lower than endo-cellulase (p-values between 5.03×10^{-7} and 9.90×10^{-7}, by one-way ANOVA; Fig. 3B). It suggests that cellulose in ENB might be shredded into short chains more readily than further hydrolysis into β-$_D$-glucose, yet the highly active γ-amylase was able to produce β-$_D$-glucose from starch. Hemicellulose- hydrolyzing enzymes displayed a pattern similar to cellulose-hydrolyzing enzymes, in that the enzymes for shredding hemicellulose into short chains were also more active than those detaching the short chains into free monosaccharide units.

During days 0–45, the content of protopectins decreased (p-value = 1.39×10^{-7}, by one-way ANOVA), whereas water-soluble pectins increased (p-value = 2.38×10^{-7}, by one-way ANOVA), and the sum of the two was similar (p- values between 0.133 and 0.770, by one-way ANOVA). It suggests that protopectins were solubilized but not eventually consumed during this period. Protopectins and water- soluble pectins both decreased greatly after 45 days (p-value = 2.35×10^{-4} and 1.31×10^{-6}, respectively, by one-way ANOVA), which means that a substantial catabo- lism of pectins took place. Four proteins of *M*. *importuna* were identified as pectin lyases, which appeared to partici- pate in the observed pectin degradation.

Free disaccharides and monosaccharides except fruc- tose accumulated over the first 45 days and then decreased (Fig. 3A; Supporting Information Table S5). The temporary accumulation might be due to very active shredding of polysaccharide chains while further catabo- lism was not fast enough to consume the intermediates.

Lipid degradation

Lipase activity was the second highest in ENB (Fig. 3B), suggesting that grain fats can act as a potential source of C. As lipases encoded by non-CAZy genes were absent from the metaproteomic profiles, the lipase activ- ity detected in ENB was likely contributed by the CE5 proteins (Martinez *et al*., 1994; Nakamura *et al*., 2017) of *M*. *importuna* (Fig. 4). However, lipids were not a major C source in ENB, due to their low content. Crude fats and triglycerides both accumulated during days 15–45 (Fig. 3A; p-value = 2.86×10^{-6} and 3.93×10^{-6}, respectively, by one-way ANOVA), indicating that lipids were synthesized and stored in ENB temporarily. After 45 days, net consumptions of crude fats and triglycerides were both significant (p-value = 1.40×10^{-5} and 5.10×10^{-4}, respectively, by one-way ANOVA), suggesting that excess of C nutrients could be converted to lipid stock and consumed later. Noticeably, the triglyceride amount per ENB at day 75 was still higher than the start (day 75 > day 0, p-value = 0.001, by one-way ANOVA).

Lignin decomposition

Lignin decomposition took place rarely during days 0–15 (p-value = 0.963, by one-way ANOVA), slowly during days 15–45 (p-value = 0.019, by one-way ANOVA) and faster during days 45–75 (p-value = 4.98×10^{-6}, by one- way ANOVA; Fig. 3A). Over the 75 days, the ratios among total p-hydroxyphenyl (H), total syringyl (S) and total guaiacyl (G) units changed less than their free monomers (Supporting Information Table S5). The ratio of S:G (total units) decreased during days 0–45 and then increased during days 45–75 (Supporting Information Table S5). Free H and free G monomers as well as free ferulic acid were rapidly consumed during days 0–15 (p- value = 7.43×10^{-12}, 1.28×10^{-9} and 2.24×10^{-12}, respectively, by one-way ANOVA), unlike the significantly accumulated free S monomer (p-value = 1.06×10^{-10}, by one-way ANOVA). During days 15–75, free S and free G monomers both decreased (p-value = 4.76×10^{-11} and 0.002, respectively, by one-way ANOVA) (Supporting Information Table S5). The enzymes involved in oxidative breakdown of lignin showed low activities (Fig. 3B). Mn peroxidase (oxidizing Mn^{2+} to Mn^{3+}) and versatile peroxidase (oxidizing veratryl alcohol) had much lower activities than laccase (p-values between 3.63×10^{-6} and 8.56×10^{-4}, by one-way ANOVA).

Although the *M*. *importuna* SCYDJ1-A1 genome pos- sesses several genes predicted as lignin-degrading enzymes, only a laccase-like multicopper oxidase (LMCO)

Fig. 3. A. Content change of major chemicals in ENB at day 0, 15, 45 and 75. The values of the chemical contents are mean of three biological replicates, with standard deviation bars. All the values, as well as pH and water content in ENB, are presented in the Supporting Information Table S5. B. Enzymatic activities in ENB, measured at the pH and temperature of ENB at the sampling date. A subset of the figure with the verti- cal axis zoomed in is shown to display low activity enzymes. Enzymatic activity which might be contributed by both CAZymes and non-CAZymes is labelled with empty diamond, whereas the activity completely unrelated with CAZymes is labelled with solid diamond. The activity level is mean of three biological replicates, with standard deviation bars. Significant difference in multi-group comparison of an item at the three time-points was judged by one-way ANOVA. Significant difference in pairwise comparison of two items at the same time-point, or during the same period, was judged by *t* test. A full list of all *p*-values is provided in Supporting Information Table S8.

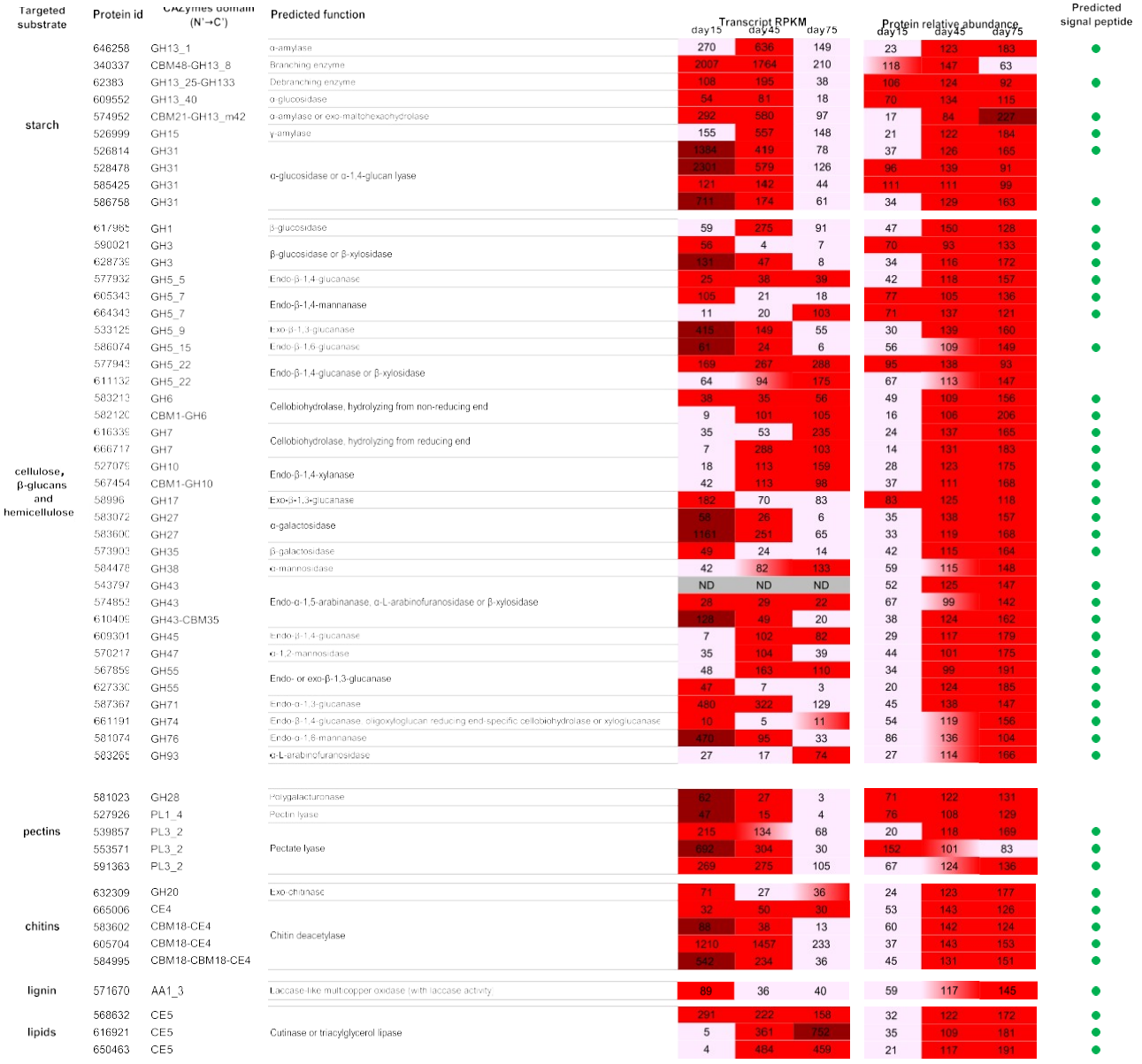

Fig. 4. Major CAZymes of *M. importuna* SCYDJ1-A1 involved in ENB decomposition. A supplemental figure showing all 88 CAZymes identified in ENB is provided in Fig. S5. Expression levels of transcripts and proteins were estimated by RNA-Seq and nanoLC-MS/MS respectively. Steady-state transcript level (in RPKM) and protein relative abundance are the mean of three biological replicates. ND, not detected. Functions of CAZymes were predicted according to their nearest analogues whose activities had been characterized in previ- ous studies, as provided by the CAZy database. Fold-change in RPKM between time-points, together with *p*-value of pairwise comparison, was calculated by the Baggerly's proportion-based test (Baggerly *et al.*, 2003) with a FDR correction for multiple testing (Benjamini and Hochberg, 1995). Fold-change values of protein relative abundance between time-points, together with *p*-value of pairwise compari- son, were calculated by *t* test with FDR correction. Significant upregulation and downregulation were judged by fold-change > 2 and fold-change < 0.5, respectively, whereas FDR-corrected *p*-value < 0.05. Fold-change values and *p*-values are provided in Supporting Infor- mation Table S8. [Color figure can be viewed at wileyonlinelibrary.com]

of AA1_3 family was detected in the metaproteomic pro- files (Fig. 4), supporting the observed enzymatic activity. The laccase activity of the AA1_3 LMCO protein has been verified by biochemical characterization of the purified enzyme (Zhang *et al*., 2019). The activity levels at day 45 and day 75 were both higher than day 15 (p- value = 6.52×10^{-6} and 2.74×10^{-7}, respectively, by one-way ANOVA; Fig. 3B). This trend is consistent with the significant lignin degradation taking place dur- ing days 45–75 (p-value = 4.98×10^{-6}, by one-way ANOVA; Fig. 3A) and is also supported by increased abundance of the AA1_3 LMCO protein in ENB (Fig. 4).

N nutrition

Inorganic ammonium and nitrate represented a minor pro- portion in the total N (Supporting Information Table S5), most N being incorporated in organic compounds. The amounts of soluble proteins and free amino acids at day 75 were all higher than the start (p-value = 2.59×10^{-5} and 1.94×10^{-7}, respectively, by one-way ANOVA). Total proteins reached the highest content at day 15. Soluble proteins showed a continuous increase during days 0–45 (days 0–15: p-value = 9.95×10^{-4}; days 15–45: p- value = 0.001, by one-way ANOVA). Free amino acids were initially consumed during days 0–15 (p-value = 0.001, by one-way ANOVA) and then accumulated after 15 days (day 45 > day 15, p-value = 6.84×10^{-4}; day 75 > day 45, p-value = 2.59×10^{-7}, by one-way ANOVA). These results suggest that *M. importuna* mycelium colonizing ENB, possibly together with other microbes, used some of the free amino acids and borrowed some additional N from the environment in the early period, which was likely used to manufacture the large quantity of enzymes involved in substrate decomposition. This contention was confirmed by an elemental-tracing experiment with ^{15}N isotopic label- ling of soil N, showing that ENB was indeed acquiring N from the underneath soil over the first 15 days, and the assimilated N was further enriched into the soluble pro- teins in ENB (Supporting Information Fig. S4). In the late period, lysis of dead microbial cells, as well as breakdown of proteins, might release free amino acids as well as ammonium into ENB substrate. Enzymes involved in N scavenging from proteins and chitins showed low activities in ENB (Fig. 3B), suggesting that degradation of proteins and chitins seemed not very active.

Expression of CAZymes

ENB was colonized by *M. importuna* mycelium and a cor- tege of environmental microorganisms. *M. importuna*, together with 10 of the most abundant fungal genera (*Mor- tierella*, *Trichoderma*, *Monodictys*, *Peziza*, *Cladosporium*,

Neonectria, *Penicillium*, *Fusarium*, *Oliveonia* and *Plectosphaerella*), were defined as the major fungal taxa in ENB. They represented 96.5% of the fungal community, as determined by metabarcoding survey (see *Changes in the microbial community* section).

Enzymes broadly characterized as hemicellulases and pectinases (i.e., ß-xylosidases, endo-ß-1,6-glucanases, polygalacturonases, pectin lyases and mannanases) were among the most highly transcribed genes at day 15. Com- plete breakdown of ENB substrate requires joint efforts from multiple enzymes of GH, CE, PL and AA families. At day 45, genes coding for α- and γ-amylases, GH13_8 branching enzyme and α-glucosidase/ α-1,4-glucan lyase were transcribed at a higher level. Cutinase/lipase, lytic polysaccharide monooxygenases (LPMOs) and expansin- related proteins showed a higher transcription level at the later stage (Supporting Information Fig. S5).

A total of 1380 proteins belonging to *M*. *importuna* plus the other 10 major fungal taxa in ENB were identified by 2D nanoLC-MS/MS, among which 60% (833) were from *M*. *importuna*. The 833 proteins represented 7% of the 11 971 predicted genes in the morel genome. This set included 88 CAZymes (24% of a total of 360 CAZy-genes in the *M*. *importuna* SCYDJ1-A1 genome), and few were encoded by other fungi (Supporting Information Table S6). CAZymes expressed by *M*. *importuna* included 47 GH, 11 CE, 4 PL, 17 AA and 5 GT (Fig. 4). The diverse array of CAZymes, including hydrolytic and redox enzymes, pointed to the multiple pathways and degradative mechanisms involved in ENB decomposition. During days 15–45,
168 out of the 833 morel proteins were upregulated, whereas 5 were downregulated (Supporting Information Fig. S6). Over a half of the 88 CAZy-proteins were upregulated during this period, confirming a striking activa- tion of the decay apparatus in ENB. Eighty eight out of the 833 morel proteins were downregulated during days 45–75. It reflected the decline of *M*. *importuna* mycelium in ENB during the late period, as evidenced by the fungal commu- nity profiles (Fig. 5). However, an overwhelming majority
(86) of the 88 CAZy-proteins remained at a constant level during days 45–75 (Supporting Information Fig. S6).

Changes in the microbial community

The bacterial and fungal communities in ENB at 15, 45 and 75 days were surveyed, respectively, through metabarcoding of bacterial 16S ribosomal DNA (rDNA) and fungal internal transcribed spacer (ITS). The bacterial and fungal communities both showed a growing trend in their taxonomic richness (i.e., the observed number of operational taxonomic unit (OTU), ACE and Chao1) and diversity (i.e., the Shannon–Wiener and Inverse Simpson's indices) during ENB decomposition (Table 1). Richness of bacterial communities was higher than the fungal

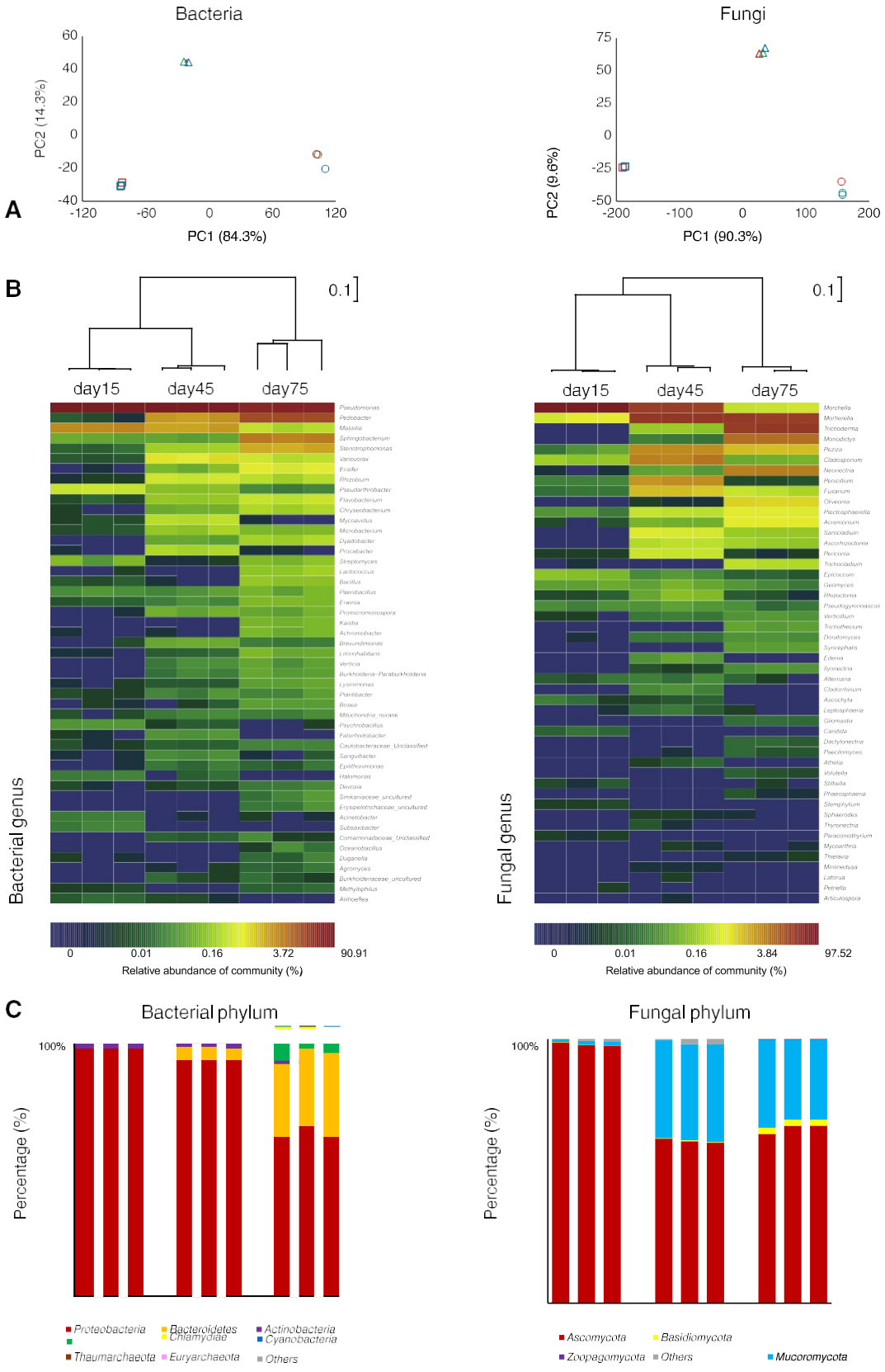

Fig. 5. Legend on next page.

communities at every time-point. Bacterial OTU richness was similar at day 15 and day 45 but increased signifi- cantly at day 75. The fungal OTU richness increased mostly during days 15–45, suggesting that an increasing number of fungal taxa colonized ENB at this stage.

PCA and hierarchical clustering showed that both bac- terial and fungal communities were quite distinct between different time-points (Fig. 5A and B). Community compo- sition at genus (Fig. 5B) and phylum (Fig. 5C) levels were both uneven in taxonomic abundance. *Pseudomonas* was always the overwhelmingly major bacterial group. As mentioned above, *M*. *importuna* and 10 other abundant genera (belonging to 15 OTUs) represented 96.5% of the fungal community in ENB. *M*. *importuna* was dominant at day 15 and was greatly overturned by *Trichoderma*, *Mortierella* and a few other taxa during days 45–75.

Discussion

Saprotrophic fungi can degrade soil polysaccharides using a versatile arsenal of catabolic enzymes including GH, CE, PL and AA, which are classified in the CAZy database (http://www.cazy.org) (Lombard *et al*., 2014). Compared with the genomes of other taxonomically related Pezizomycetes (Fig. 6), the two strains of *M*. *importuna* were characterized by an under-represented set of CAZy-genes involved in lignin decomposition and an over-represented set of CAZy-genes degrading pec- tins. In comparison with commercially cultivated Basidiomycota mushrooms *L*. *edodes*, *P*. *ostreatus* and *A*. *bisporus*, *M*. *importuna* SCYDJ1-A1 genome encodes over-represented sets of CAZy-genes involved in lipid and pectin degradation and an under-represented set of CAZy-genes involved in lignin decomposition (Supporting Information Fig. S7A). Indeed, *L*. *edodes* (Gaitán- Hernández *et al*., 2011; Cai *et al*., 2017) and *P*. *ostreatus* (Isikhuemhen and Mikiashvilli, 2009) have been reported to produce high levels of laccase and Mn peroxidase activities thereby degrading lignin as one of their major C sources. In contrast, *M*. *importuna* grows on deeply decomposed plant biomass such as soil and plant-litter compost. It is supported by the results of biochemical assays, which revealed that *M*. *importuna* possesses decomposition capabilities adapted to polysaccharides over lignin.

In the genome of *M*. *importuna* SCYDJ1-A1, cellulose- and hemicellulose-hydrolyzing enzymes are encoded by

over a dozen of GH genes, but the observed activities were not as high as amylases. In comparison, the single *M*. *importuna* GH15 protein contributed to a higher level of γ-amylase activity. This finding suggests that gene copy number and proteomic profiling should be completed by measurements of enzymatic activities to provide a comprehensive portrait of the decomposition mechanisms. High amylase activity has been reported in saprotrophic moulds such as *Aspergillus* and *Mucor* (Saranraj and Stella, 2013; Gopinath *et al*., 2017) but was rarely described in mushrooms. High activity levels of enzymes hydrolyzing lipids and pectins were also observed in ENB during the decomposition. Pectin solubilization could disintegrate lignocellulosic complex and enhance accessibility to microbes and enzymes (Shirkavand *et al*., 2016).

The substantial expression of redox enzymes provides additional insight into ENB degradative processes. Compared with the Basidiomycota mushrooms *P*. *ostreatus* and *A*. *bisporus*, *M*. *importuna* SCYDJ1-A1 displayed a pattern of expressed CAZy-proteins with obvious shortage in laccase (AA1), Mn peroxidase and versatile peroxidase (AA2), as well as glyoxal oxidase (AA5) essential for generating H_2O_2 (Supporting Information Fig. S7B), supporting the limited decomposition activities against lignin. Two copies of AA1_3 LMCO were identified in the *M*. *importuna* SCYDJ1-A1 genome, but only one was expressed in ENB. Similar results were observed in the sclerotium in mushroom spawn, the surface-soil mycelium before and after contact with ENB as well as in primordium and fruiting body of *M*. *importuna* SCYDJ1-A1 (Zhang *et al*., 2019). As laccase attacks mainly phenolic units while Mn peroxidase and versatile peroxidase are much more effective on non-phenolic units (Janusz *et al*., 2017), the much higher laccase activity compared with Mn peroxidase and versatile peroxidase suggests that phenolic-unit components might be degraded faster than non-phenolic components. ENB decomposition by *M*. *importuna* caused the ratio of total S:G to increase initially and then fall, differs with *A*. *bisporus* that induced a continuous increase in the total S:G ratio during its entire vegetative growth in cultivation substrate (Kabel *et al*., 2017). Concerning the other redox enzymes, Cu-dependent LPMO has been shown to stimulate the performance of endo- and exo-cellobiohydrolases (Vaaje-Kolstad *et al*., 2010). The high transcription of benzoquinone reductase (AA6) during days 15–45 is consistent with a role of

Fig. 5. Changes in the microbial communities colonizing ENB.
A. PCA analyses of bacterial and fungal communities in ENB at day 15 (empty squares), day 45 (empty triangles) and day 75 (circles), with three replicates for each time-point coloured in red, green and blue respectively.
B. Relative abundance of bacterial and fungal genera, with hierarchical clustering tree constructed based on community similarity. Only the top 50 prominent genera are shown here.
C. Relative abundance of bacterial and fungal phyla in ENB at day 15, 45 and 75.

iversity of the bacterial and fungal communities in ENB at days 15, 45 and 75.

ommunity	ampling time	)TU coverage		annon-Wiener diversity	erse Simpson's diversity
		Replicate	Identified OTU	ACE richness	hao1 richness
	Day 45				
	Day 75				
Fungal	Day 15				
	Day 45				
	Day 75				

amples had an OTU coverage above 0.999, showing that the sampling had sufficient scales. OTUs were clustered at 97% similarity. The 95% lower and upper confidence limits are presented in parentheses.

hydroxyl radicals in ENB decomposition (Cassagnes *et al*., 2015). In addition to plant-polysaccharide degradation, chi- tins constructing fungal cell walls are likely a substrate for chitin deacetylases (CBM18-CE4). The high transcription of chitin metabolism-related genes at day 15 might reflect early colonization of ENB by morel mycelium. The *M*. *importuna* SCYDJ1-A1 genome possesses two copies of GH131 gene, a hallmark of plant-tissue-colonizing fungi (Anasontzis *et al*., 2019), but none was likely expressed as an enzymatic protein during ENB decomposition, although their transcriptions were indeed observed.

The microbiota in ENB showed low OTU richness as well as low diversity, as compared with soil environmen- tal samples (Tan *et al*., 2013; Calderón *et al*., 2016), composts (Wang *et al*., 2018), water (Thaler *et al*., 2017) and guts (Griffin *et al*., 2017). It means that the decaying ENB hosted a microbiota of limited complexity, compara- ble to that of seed endophytic microbiota (Barret *et al*., 2015), with a similar feature that their relative abun- dances of microbial taxa were quite uneven. For instance, the overwhelmingly high proportion of pseudo-monads in the bacterial communities in ENB lasted for the entire course of morel cultivation. Biofilms of soil- borne pseudomonads around hyphae are known for sev- eral mushrooms, such as *P*. *ostreatus* (Cho *et al*., 2003), *Laccaria bicolor* (Deveau *et al*., 2007), *A*. *bisporus* and *Tuber borchii* (Frey-Klett *et al*., 2011). Farming of *P*. *putida* by *M*. *crassipes* has been reported (Pion *et al*., 2013). *M*. *importuna* might tend to enrich pseudomonad cohabitants as well.

Decline of *M*. *importuna* mycelium in ENB during days 45–75 was reflected by its relative abundance in the fun- gal communities, but the CAZy-proteins produced by *M*. *importuna* mycelium were durable enough to retain in ENB until day 75, given that most of the expressed CAZy-proteins were quantified similarly at day 45 and day 75. This is also supported by the patterns of enzy- matic activities, all of which not decreased from day 45 to day 75. The increase in surface soil total organic C as well as increased fruiting body yield, during the 45 to 75 days period (Fig. 2A), indicated that ENB still had a positive effect on fruiting in the late phase. Only by retaining the ENBs to contact with the mushroom bed for at least 75 days, can

the dry weight of fruiting body yield reach the average level in agricultural pro- duction reported previously (Liu *et al*., 2018). The com- pounds resulting from ENB decomposition are likely exported to the mushroom bed via mycelial networks, as well as free diffusion and running-off. Besides creat- ing a surface soil with enhanced organic C content, ENB caused N level in the mushroom bed to fall tem- porarily during days 0–15 and restore later. Interest- ingly, decaying plant litter had similar effects to

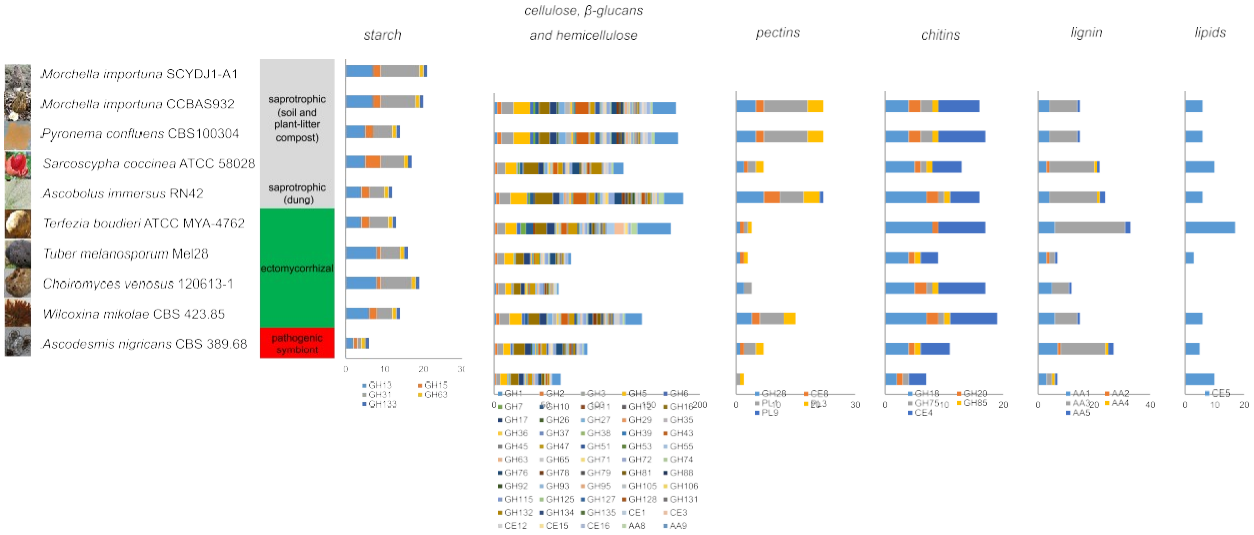

Fig. 6. Distribution and occurrence of genes coding for CAZymes involved in decomposition of plant polysaccharides, lignin and lipids. The genomes of the two *M. importuna* strains SCYDJ1-A1 and CCBAS932 are compared with taxonomically related Pezizomycetes. The CAZy- genes are sorted in categories according to their known targeted substrate. Significant over-representation and under-representation of CAZy- genes in different categories of targeted substrates were estimated by Fisher's exact test, with the statistical data shown in Supporting Informa- tion Table S7. Pictures of the fungi are derived from the homepages of the species in the JGI genome portals.

enhance soil organic C content and induce a migration of soil N towards the decaying plant litter (Hori *et al*., 2018). In this context, the man-made ENB in contact with the mushroom bed plays a role that could mimic the effects of plant litter, which is often abundant in natural ecosystems such as forests and grasslands. Interpretation of ENB decomposition by *M. importuna* might provide insights into the mechanisms triggering

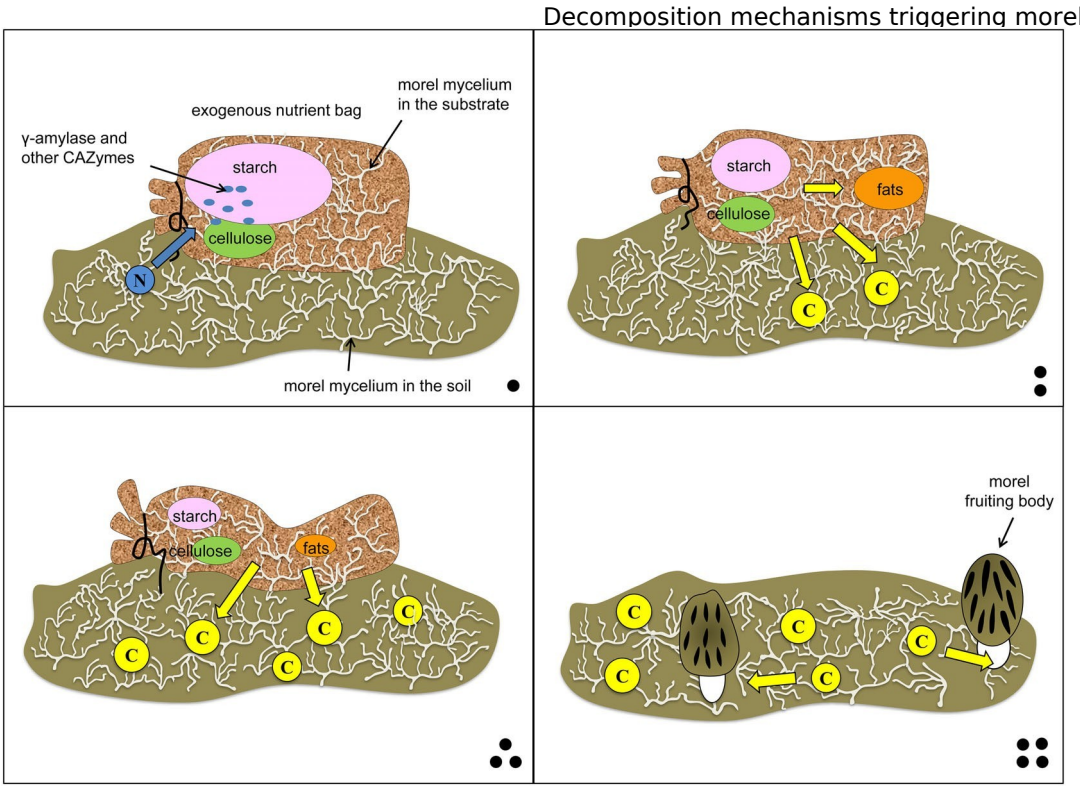

Fig. 7. Schematic diagram of ENB decomposition by *M. importuna* SCYDJ1-A1.

wild saprotrophic mushrooms fruiting from soils, which might advance potential attempts to domesticate more species of wild saprotrophic mushrooms to artificial cultivation.

Conclusions

During *M*. *importuna* cultivation, the vegetative mycelium colonizing ENB substrate releases a complex set of deg- radative CAZymes to efficiently decompose and metabo- lize polysaccharides, such as starch and cellulose from wheat grains and rice husks (Fig. 7). The metabolites released by this decay mechanism are exported to the adjacent surface soil of the mushroom bed, triggering and sustaining fruiting of morels.

Experimental procedures

Morel strain

The cultivable black morel strain, *M*. *importuna* SCYDJ1-A1, is a diploid strain as used in commercial application. It was bred from an ancestor originally col- lected in 2011, from the hilly terrain of Muerda village (31.6^0 N, 103.4^0 E, altitude 2100 m), Lixian county, Sich- uan province, China. The site belongs to the eastern part of the Qinghai–Tibetan plateau, which has a cold climate all through the year and had no forest fire for at least 10 years. The forest ecosystem from which the fruiting body was collected had a vegetative cover composed of mainly willow and shrub. The fruiting body grew in a nearly-bare soil with very little coverage of plant litter. The wild strain *M*. *importuna* CCBAS932 was collected from an oak forest in France. The fruiting body grew directly from a plant-litter compost without much soil. Haploid cul- tures of monosporal isolates from the SCYDJ1-A1 and CCBAS932 strains were used for genome sequencing.

Experimental treatments and morel cultivation

Morel cultivation in this study was carried out in a farm in Tianjiaba Village (30.5^0 N, 104.5^0 E, Yangma town, Jianyang city, Sichuan province, China). A total of 123 grids of nurs- ery bed were built in a vegetable greenhouse. Each grid was 1.5 m^2 in area, built with bricks and separated with each other. A sandy loam soil was collected from a farm nearby, thoroughly mixed to homogeneity, and evenly loaded into all the grids. Physiochemical background of the pre-homogenized soil was characterized (Supporting Infor- mation Table S4).

Fifteen grids out of the 123 were randomly selected for five treatments. In the five treatments, ENB contacted with the mushroom bed for 0, 15, 45 and 75 days or for the entire course (i.e., staying on the mushroom bed until

all fruiting bodies were harvested) respectively. Each treatment included three individual grids as three biologi- cal replicates. *M. importuna* strain SCYDJ1-A1 was culti- vated in the 15 grids, using mushroom spawn produced by Jindi-Tianlingjian company (Sichuan, China; see Supporting Information). The mushroom spawn is free from any bacterial or fungal contamination.

ENB was made by filling 350 g fresh weight of soaked wheat grains and rice husks, with a dry weight ratio of 85:15, into polypropylene casing. ENB was autoclaved at 121^0C for 3 h, which inactivated potential decomposition enzymes from cereal ingredients. Ten ENBs were placed in each grid. The ENBs were pierced in the bottom cas- ing and tightly pressed on the surface of the inoculated soil (mushroom bed) 15 days after the morel sowing. The 15 grids consisted of five different treatments of ENB last- ing time with three individual replicates for each treat- ment. For the 0 day treatment, ENBs were not placed on the soil. For the 15, 45 and 75 day treatments, ENBs were removed and sampled at day 15, day 45 and day 75 after contact with the mushroom bed respectively. Temperature inside ENB was measured with electronic thermometer sensors, recorded every 30 min, and stored automatically, throughout the entire cultivation course (Supporting Information Fig. S2).

More details about the procedures for making mush- room spawn and ENB, morel sowing and field manage- ments are provided in the Supporting Information.

Sampling

For each experimental grid, 10 ENBs were sampled at 0, 15, 45 and 75 days after contact with mushroom bed, snap frozen in liquid nitrogen, pooled and homogenized (but not milled) to generate a replicate sample. Surface soil of 0–2 cm depth was collected for chemical analysis. Soil cores (2 cm × 2 cm × 2 cm) were collected using a sterile blade, from 20 random points in each experimental grid, and pooled as a replicate. Soils of 0, 15, 45 and 75 day treatments, as well as after completion of morel harvest, were sampled respectively. For each treatment, fruiting bodies were harvested when their size reached the size-request (height, 5–8 cm; pileus length, 3–5 cm) for a commercial product in the international trade.

Biochemical assays

Chemical components in ENB substrate, fruiting body and soil samples (Supporting Information Table S5) were quantified with classical analytical methods based on spectrophotometry or high-performance liquid chromatog- raphy (HPLC). The activity of selected decomposition enzymes was measured using crude soluble proteins extracted from ENB. To investigate enzymes involved in

substrate decomposition, mostly extracellular, proteins were extracted by a soaking method (Zhu *et al*., 2016) aimed to maximize extracellular enzyme sampling (see Supporting Information), although potential contamination from intracellular proteins cannot be ruled out. Activity of enzymes listed in Fig. 3B was measured with colorimetric or HPLC method (Supporting Information Table S9). Enzy- matic activity was measured as the ability to catalyze sub- strate conversion (in milligram) per minute by the protein extracts from per gram (dry weight) of ENB. Phosphate buffer for enzymatic reaction had the same pH of the cor- respondent ENB sample, whereas assay temperature was set at the average temperature at the sampling date.

Genome sequencing, assembling and gene annotation

The genome of a monosporal haploid culture from *M*. *importuna* SCYDJ1-A1 was sequenced using a combina- tion of Illumina fragment (270 bp insert size) and 4 kb long mate-pair libraries, assembled using ALLPATHS-LG (Gnerre *et al*., 2011) and annotated using the JGI Anno- tation Pipeline (Grigoriev *et al*., 2014), as described by Murat and colleagues (2018).

RNA-Seq

Total RNA extraction, cDNA library construction and sequencing, RNA-Seq reads assembling, bioinformatic procedures for transcript profiling as well as statistical analyses in upregulation and downregulation of transcript level were carried out as described by Morin and col- leagues (2019). In brief, 1–3 μg of total RNA was extracted from the combined contents of all 10 ENBs from each experimental grid, using the RNeasy Plant Mini RNA Extraction Kit (Qiagen, Germany), and stored at -80^0 C until further analysis. cDNA library construction and sequencing were performed at the sequencing facil- ity of Beijing Genomics Institute (BGI, in Wuhan branch, China) according to standard Illumina protocols. Raw reads from paired-end sequencing were quality controlled, trimmed and mapped to the *M. importuna* SCYDJ1-A1 ref- erence transcripts (https://genome.jgi.doe.gov/Morimp1/Mor-imp1.download.html, Folder: Annotation\Filtered Models \Transcripts) to extract a *M. importuna* subset from the metatranscriptome of the target fungal community (Supporting Information Table S10), using the software pipeline of the CLC Genomics Workbench 11 (Qiagen, Ger- many). Low-quality reads with Phred-quality score < 20 or length < 50 bp were discarded. Illumina-adapter strings were removed. Alignment was performed with stringent settings (similarity and length read mapping criteria at 98% and 95%, respectively; maximum 10 hits for a read on differ- ent genes). Details about the RNA-Seq libraries, including the counts of mapped RNA-Seq reads in the ENB

metatranscriptomes at the three time-points, as well as mapping rates were presented in Supporting Information Table S11. The assembled metatranscriptomes were further analyzed using the CLC Genomics Workbench. Total mapped paired-end reads for each gene were calculated and total read counts were normalized as reads per kilo- base of gene model per million fragments mapped (RPKM; Mortazavi *et al*., 2008), which was used to estimate tran- script level of each gene. Fold-change values of the RPKM of each transcript between different time-points, together with *p*-value of pairwise comparison, were calculated by the Baggerly's proportion-based statistical test (Baggerly *et al*., 2003) implemented in the CLC Genomic Work- bench. It is a weighted t-type test designed for comparison proportion of sequence counts, with a FDR correction for multiple testing (Benjamini and Hochberg, 1995). Signifi- cant upregulation and downregulation were judged by fold-change > 2 and fold-change < 0.5, respectively, while FDR-corrected *p*-value < 0.05.

Shotgun metaproteomics

ENB proteins were analyzed by two-dimensional nano- liquid chromatography coupled with tandem mass tags labelling mass spectrometry (2D nanoLC-MS/MS) on a Q-Exactive system (Thermo Fisher Scientific) in Luming Biotechnology, Shanghai, China. Crude protein extracts were purified by trichloroacetic acid precipitation and ace- tone washing, re-solubilized with urea and quantified as previously described (Hori *et al*., 2018). The proteins were digested with trypsin and labelled with isotopic tags as pre-vious described by Wiśniewski and colleagues (2009). Nine different tags were assigned to the 3 × 3 individual replicate samples. Peptide fragments were first separated by reverse-phase HPLC using an Agilent Zorbax Extend C18 column on an Agilent 1100 HPLC system (Agilent Technol-ogies) with a flow rate at 300 µl min^{-1}. Wavelength of UV- detector was 210 and 280 nm. Phase A: acetonitrile-H_2O (2%:98%, v/v). Phase B: acetonitrile-H_2O (90%:10%, v/v). Gradient elution steps: 0–8 min, 98% A; 8–8.01 min, 98%–95% A; 8.01–38 min, 95%–75% A; 38–50 min, 75%–60% A; 50–50.01 min, 60%–10% A; 50.01–60 min, 10% A; 60–60.01 min, 10%–98% A; 60.01–65 min, 98% A. The eluted products during 8–50 min were collected with 1 min interval into centrifuge tubes until the end of the gradient. Further separation was carried out using an Acclaim Pepmap RSLC analytical column (C18, 2 µm, 100 Å, 75 µm × 15 cm, Dionex) with a flow rate at 300 nl min^{-1}. Phase A: H_2O-FA (99.9%:0.1%, v/v). Phase B: acetonitrile-H_2O-FA (80%:19.9%:0.1%, v/v/v). Gradient elution steps: 0–55 min, 8% B; 55–79 min, 30% B; 79–80 min, 50% B;
80–90 min, 100% B. The eluted fragments were scanned in MS1 with resolution 70 000 and *m/z* range 300–1800,

followed by MS/MS fragmentation of 10 most intense pep- tide fragments detected in the MS1. The MS/MS fragmen- tation was scanned with resolution 17 500, dynamic exclusion time 30 s.

Raw data were loaded into Proteome Discoverer software v2.2 (Thermo Fisher Scientific) for protein identification and quantification, with an FDR < 1%. A total of 6030 peptide fragments were obtained in the MS/MS spectra, mapped to the user-defined reference genomes (Supporting Informa- tion Table S10). Protein hits belonging to wheat and rice, which are ingredients of ENB substrate (wheat grains and rice husks), were identified as substrate background to be manually removed. The identified proteins must have a Sequest HT score > 0 and unique peptide ≥ 1, as the criteria previously adopted by Zhu and colleagues (2016) and Cai and colleagues (2017). Fold-change values of pro- tein relative abundance between time-points, together with *p*-value of pairwise comparison, were calculated by *t* test with FDR correction. Significant upregulation and down- regulation were judged by fold-change > 2 and fold-change < 0.5, respectively, while FDR-corrected *p*-value < 0.05.

Microbiome metabarcoding

Metabarcoding survey on microbial diversity in ENB was carried out using PCR amplicons of 16S rDNA V4-V5 region for bacterial community and ITS region for fungal community. Total microbial DNA in ENB was isolated with a CTAB extracting method (Tan *et al*., 2013). V4-V5 region of bacterial 16S rRNA gene fragment was amplified with primers 515F (5^0-GTGCCAGCMGCCGCGG-3^0) and 907R (5^0-CCGTCAATTCMTTTRAGTTT-3^0; Jiang *et al*., 2017). Fungal ITS region was amplified with primers ITS1-F (5^0-CTTGGTCATTTAGAGGAAGTAA-3^0) and ITS2-R (5^0- GCTGCGTTCTTCATCGATGC-3^0) (French *et al*., 2017).

Sequencing library was constructed from the PCR amplicons, with index codes added, using NEB NextUltra DNA Library Prep Kit for Illumina (NEB) following manufac- turer's recommendations. The libraries were sequenced on an Illumina MiSeq platform at the sequencing facility of BGI (Wuhan, China) according to standard Illumina protocols. The paired-end reads were quality controlled, merged by overlapping and analyzed with the QIIME pipeline (Caporaso *et al*., 2010), as described in previous studies (Barret *et al*., 2015; Awasthi *et al*., 2017). Bacterial and fun- gal OTUs were clustered at 97% similarity threshold respec- tively. Rarefaction curve of OTU was drawn to estimate sequencing coverage (Supporting Information Fig. S7). SILVA (Release 132) database of full-length sequences and taxonomy references was used for bacterial OTU clus- tering. UNITE v7.2 (Full UNITE+INSD dataset) was used for fungal OTU clustering.

Accessibility of strain and data

Cultures from *M*. *importuna* SCYDJ1-A1 are available (for non-commercial research only) on request to Jindi-Tianlingjian company, Sichuan, China. The genome of *M*. *importuna* SCYDJ1-A1 is available at the corresponding MycoCosm genome portal at DOE Joint Genome Institute (https://genome.jgi.doe.gov/ Morimp1/ Morimp1.home.html) and also at NCBI BioProject PRJNA334370 (Genbank accession number SSHS00000000.1). RNA-Seq data: NCBI BioProject PRJNA503787. Shotgun metaproteomic data: PRIDE Archive identifier PXD012086. High-throughput sequenc- ing of bacterial 16S rDNA V4-V5 and fungal ITS: NCBI Sequence Read Archive SRP162892.

Acknowledgements

This research was mainly supported by the Sichuan Science and Technology Program (Applied Fundamental Research Project, 2018JY0637, HT), the Special Fund for Agro- scientific Research in the Public Interest (201503137, ZH), the Innovative Improvement Projects of Sichuan Province (2016ZYPZ-028, WP; 2019LWJJ-009, HT; 2016LWJJ-007, HT), the Key Breeding Project of Sichuan Province (BW), and the Laboratory of Excellence ARBRE (ANR-11-LABX- 0002-01, FMM), Region Lorraine, European Regional Devel- opment Fund. Isolation of the monosporal haploid culture from *M*. *importuna* SCYDJ1-A1, preparation of genomic DNA, as well as total mRNA for Expressed Sequence Tag (EST) survey were supported by the SAAS International Cooperation Fund 2015 (HT). Special thanks to Ms Lu Xiong (internship MSc student from Sichuan Agricultural University) for her participation in the extraction and purification of the DNA and EST-RNA samples. Library construction, sequencing, assembly, and annotation of the *M*. *importuna* SCYDJ1-A1 genome were performed within the framework of the 1000 Fun- gal Genomes project by the U.S. Department of Energy Joint Genome Institute, a DOE Office of Science User Facility, and supported by the Office of Science of the U.S. Department of Energy under Contract No. DE-AC02-05CH11231. We are grateful to farmer Dafu Tian's family for providing the field experiment site and to all field technicians for their contribution. Commercial use of *M*. *importuna* SCYDJ1-A1 is currently under protection by Jindi-Tianlingjian company, Sichuan, China.

References

Anasontzis, G.E., Lebrun, M.-H., Haon, M., Champion, C., Kohler, A., Lenfant, N., *et al*. (2019) Broad-specificity GH131 β-glucanases are a hallmark of fungi and Oomycetes that colonise plants. *Environ Microbiol* (in press) https://doi. org/10.1111/1462-2920.14596.

Awasthi, M.K., Zhang, Z., Wang, Q., Shen, F., Li, R., Li, D.- S., *et al*. (2017) New insight with the effects of biochar amendment on bacterial diversity as indicators of bio- markers support the thermophilic phase during sewage sludge composting. *Bioresour Technol* 238: 589–601.

Baggerly, K.A., Morris, J.S., Wang, J., Gold, D., Xiao, L.-C., and Coombes, K.R. (2003) A comprehensive approach to the analysis of matrix-assisted laser desorption/ionization- time of flight proteomics spectra from serum samples. *Pro- teomics* 3: 1667–1672.

Barret, M., Briand, M., Bonneau, S., Préveaux, A., Valière, S., Bouchez, O., *et al*. (2015) Emergence shapes the structure of the seed microbiota. *Appl Environ Microbiol* 81: 1257–1266.

Benjamini, Y., and Hochberg, Y. (1995) Controlling the false discovery rate: A practical and powerful approach to multi- ple testing. *J R Stat Soc Ser B (Stat Meth)* 57: 289–300.

Cai, Y., Gong, Y., Liu, W., Hu, Y., Chen, L., Yan, L., *et al*. (2017) Comparative secretomic analysis of lignocellulose degradation by *Lentinula edodes* grown on microcrystal- line cellulose, lignosulfonate and glucose. *J Proteomics* 163: 92–101.

Calderón, K., Spor, A., Breuil, M.-C., Bru, D., Bizouard, F., Violle, C., *et al*. (2016) Effectiveness of ecological rescue for altered soil microbial communities and functions. *ISME J* 11: 272–283.

Caporaso, J.G., Kuczynski, J., Stombaugh, J., Bittinger, K., Bushman, F.D., Costello, E.K., *et al*. (2010) QIIME allows analysis of high-throughput community sequencing data. *Nat Meth* 7: 335–336.

Cassagnes, L.-E., Perio, P., Ferry, G., Moulharat, N., Antoine, M., Gayon, R., *et al*. (2015) In cellulo monitoring of quinone reductase activity and reactive oxygen species production during the redox cycling of 1,2 and 1,4 qui- nones. *Free Radic Biol Med* 89: 126–134.

Chang, S.-T., and Hayes, W.A. (2013) *The Biology and Cul- tivation of Edible Mushrooms*: New York, NY: Academic Press.

Cho, Y.-S., Kim, J.-S., Crowley, D.E., and Cho, B.-G. (2003) Growth promotion of the edible fungus *Pleurotus ostreatus* by fluorescent pseudomonads. *FEMS Microbiol Lett* 218: 271–276.

Deveau, A., Palin, B., Delaruelle, C., Peter, M., Kohler, A., Pierrat, J.C., *et al*. (2007) The mycorrhiza helper *Pseudo- monas fluorescens* BBc6R8 has a specific priming effect on the growth, morphology and gene expression of the ectomycorrhizal fungus *Laccaria bicolor* S238N. *New Phytol* 175: 743–755.

Du, X.-H., Zhao, Q., and Yang, Z.-L. (2015) A review on research advances, issues, and perspectives of morels. *Mycology* 6: 1–8.

French, K.E., Tkacz, A., and Turnbull, L.A. (2017) Conversion of grassland to arable decreases microbial diversity and alters community composition. *Appl Soil Ecol* 110: 43–52.

Frey-Klett, P., Burlinson, P., Deveau, A., Barret, M., Tarkka, M., and Sarniguet, A. (2011) Bacterial-fungal inter- actions: Hyphens between agricultural, clinical, environ- mental, and food microbiologists. *Microbiol Mol Biol Rev* 75: 583–609.

Gaitán-Hernández, R., Esqueda, M., Gutiérrez, A., and Beltrán-García, M. (2011) Quantitative changes in the bio- chemical composition of lignocellulosic residues during the vegetative growth of *Lentinula edodes*. *Braz J Microbiol* 42: 30–40.

Gnerre, S., MacCallum, I., Przybylski, D., Ribeiro, F.J., Burton, J.N., Walker, B.J., *et al*. (2011) High-quality draft

assemblies of mammalian genomes from massively paral- lel sequence data. *Proc Natl Acad Sci U S A* 108: 1513–1518.

Gopinath, S.C., Anbu, P., Arshad, M., Lakshmipriya, T., Voon, C.H., Hashim, U., and Chinni, S.V. (2017) Biotechnological processes in microbial amylase production. *Biomed Res Int* 2017: 1–9. https://doi.org/10.1155/2017/1272193.

Griffin, N.W., Ahern, P.P., Cheng, J., Heath, A.C., Ilkayeva, O., Newgard, C.B., *et al*. (2017) Prior dietary practices and connections to a human gut microbial metacommunity alter responses to diet interventions. *Cell Host Microbe* 21: 84–96.

Grigoriev, I.V., Nikitin, R., Haridas, S., Kuo, A., Ohm, R., Otillar, R., *et al*. (2014) MycoCosm portal: Gearing up for 1000 fungal genomes. *Nucleic Acids Res* 42: D699–D704. Hobbie, E.A., Rice, S.F., Weber, N.S., and Smith, J.E. (2016) Isotopic evidence indicates saprotrophy in post-fire *Morchella* in Oregon and Alaska. *Mycologia* 108: 638–645. Hori, C., Gaskell, J., Cullen, D., Sabat, G., Stewart, P.E., Lail, K., *et al*. (2018) Multi-omic analyses of extensively decayed *Pinus contorta* reveal expression of a diverse array of lignocellulose-degrading enzymes. *Appl Environ Microbiol* 84: e01133–e01118.

Isikhuemhen, O.S., and Mikiashvilli, N.A. (2009) Lignocellulolytic enzyme activity, substrate utilization, and mushroom yield by *Pleurotus ostreatus* cultivated on sub- strate containing anaerobic digester solids. *J Ind Microbiol Biotechnol* 36: 1353–1362.

Janusz, G., Pawlik, A., Sulej, J., Świderska-Burek, U., Jarosz-Wilkołazka, A., and Paszczyn‚ski, A. (2017) Lignin degrada- tion: Microorganisms, enzymes involved, genomes analysis and evolution. *FEMS Microbiol Rev* 41: 941–962.

Jiang, Y., Li, S., Li, R., Zhang, J., Liu, Y., Lv, L., *et al*. (2017) Plant cultivars imprint the rhizosphere bacterial community composition and association networks. *Soil Biol Biochem* 109: 145–155.

Kabel, M.A., Jurak, E., Mäkelä, M.R., and de Vries, R.P. (2017) Occurrence and function of enzymes for lignocellulose degradation in commercial *Agaricus bisporus* cultiva- tion. *Appl Microbiol Biotechnol* 101: 4363–4369.

Larson, A.J., Cansler, C.A., Cowdery, S.G., Hiebert, S., Furniss, T.J., Swanson, M.E., and Lutz, J.A. (2016) Post-fire morel (Morchella) mushroom abundance, spatial structure, and harvest sustainability. *For Ecol Manage* 377: 16–25.

Liu, Q., Ma, H., Zhang, Y., and Dong, C. (2018) Artificial cul- tivation of true morels: Current state, issues and perspec- tives. *Crit Rev Biotechnol* 38: 259–271.

Liu, S.-L., Li, K.-B., Zhu, H., Lin, J.-X., Shi, C.-H., Zhou, J., *et al*. (2016) The current situation of *Morchella* artificial cultivation technology and problem analysis. *Edible Med Mushrooms* 24: 290–293.

Lombard, V., Ramulu, H.G., Drula, E., Coutinho, P.M., and Henrissat, B. (2014) The carbohydrate-active enzymes database (CAZy) in 2013. *Nucleic Acids Res* 42: D490–D495.

Martin, J., Han, C., Gordon, L.A., Terry, A., Prabhakar, S., She, X., *et al*. (2004) The sequence and analysis of duplication-rich human chromosome 16. *Nature* 432: 988–994.

Martinez, C., Nicolas, A., van Tilbeurgh, H., Egloff, M.P., Cudrey, C., Verger, R., and Cambillau, C. (1994)

Cutinase, a lipolytic enzyme with a preformed oxyanion hole. *Biochemistry* 33: 83–89.

Masaphy, S. (2010) Biotechnology of morel mushrooms: Successful fruiting body formation and development in a soilless system. *Biotechnol Lett* 32: 1523–1527.

Morin, E., Miyauchi, S., San Clemente, H., Chen, E.C.H., Pelin, A., de la Providencia, I., *et al*. (2019) Comparative genomics of *Rhizophagus irregularis*, *R. cerebriforme*, *R. diaphanus* and *Gigaspora rosea* highlights specific genetic features in Glomeromycotina. *New Phytol* 222: 1584–1598.

Mortazavi, A., Williams, B.A., McCue, K., Schaeffer, L., and Wold, B. (2008) Mapping and quantifying mammalian transcriptomes by RNA-Seq. *Nat Meth* 5: 621–628.

Murat, C., Payen, T., Noel, B., Kuo, A., Morin, E., Chen, J., *et al*. (2018) Pezizomycetes genomes reveal the molecu- lar basis of ectomycorrhizal truffle lifestyle. *Nat Ecol Evol* 2: 1956–1965.

Nakamura, A.M., Nascimento, A.S., and Polikarpov, I. (2017) Structural diversity of carbohydrate esterases. *Bio- technol Res Innov* 1: 35–51.

O'Donnell, K., Rooney, A.P., Mills, G.L., Kuo, M., Weber, N. S., and Rehner, S.A. (2011) Phylogeny and historical bio- geography of true morels (*Morchella*) reveals an early Cretaceous origin and high continental endemism and provincialism in the Holarctic. *Fungal Genet Biol* 48: 252–265.

Ower, R.D., deceased, Mills, G.L. and Malachowski, J.A., *Inventors; Neogen Corporation, assignee. Cultivation of morchella*. United States patent US4,866,878. 19 Sep 1989. Peng, W., Tang, J., He, X., Chen, Y., and Tan, H. (2016) Status analysis of morel artificial cultivation in Sichuan. *Edible Med Mushrooms* 24: 145–150.

Pilz, D., Weber, N.S., Carol Carter, M., Parks, C.G., and Molina, R. (2004) Productivity and diversity of morel mushrooms in healthy, burned, and insect-damaged for- ests of northeastern Oregon. *For Ecol Manage* 198: 367–386.

Pilz, D., McLain, R., Alexander, S., Villarreal-Ruiz, L., Berch, S., Wurtz, T.L., *et al*. (2007) *Ecology and Manage- ment of Morels Harvested from the Forests of Western North America*. Corvallis: General Technical Report: For- est Service, Pacific Northwest Research Station, United States Department of Agriculture.

Pion, M., Spangenberg, J.E., Simon, A., Bindschedler, S., Flury, C., Chatelain, A., *et al*. (2013) Bacterial farming by the fungus *Morchella crassipes*. *Proc R Soc B Biol Sci* 280: e2242.

Roze, M.E. (1882) Adherence de la base d'appareils asco- spores de *Morchella* Sur *Helianthus tuberosus*. *Bull Soc Bot France* 19: 166–167.

Saranraj, P., and Stella, D. (2013) Fungal amylase—A review. *Int J Microbiol Res* 4: 203–211.

Shirkavand, E., Baroutian, S., Gapes, D. J., and Young, B. R. (2016) Combination of fungal and physico- chemical processes for lignocellulosic biomass pre- treatment – A review. *Renew Sust Energ Rev* 54: 217–234.

Stojkovi‚c, D., Reis, F.S., Barros, L., Glamo~clija, J., C‚ iri‚c, A., van Griensven, L.J.I.D., *et al*. (2013) Nutrients and non-

nutrients composition and bioactivity of wild and cultivated *Coprinus comatus* (O.F.Müll.) Pers. *Food Chem Toxicol* 59: 289–296.
Tan, F.-H. (2016) History, current station and prospect of morel cultivation. *Edible Med Mushrooms* 24: 140–144.
Tan, H., Barret, M., Mooij, M.J., Rice, O., Morrissey, J.P., Dobson, A.D., *et al*. (2013) Long-term phosphorus fertilisation increased the diversity of the total bacterial community and the *phoD* phosphorus mineraliser group in pasture soils. *Biol Fertil Soils* 49: 661–672.
Thaler, M., Vincent, W.F., Lionard, M., Hamilton, A.K., and Lovejoy, C. (2017) Microbial community structure and interannual change in the last epishelf lake ecosystem in the north polar region. *Front Mar Sci* 3: e275.
Tietel, Z., and Masaphy, S. (2018) Aroma-volatile profile of black morel (*Morchella importuna*) grown in Israel. *J Sci Food Agric* 98: 346–353.
Vaaje-Kolstad, G., Westereng, B., Horn, S.J., Liu, Z., Zhai, H., Sørlie, M., and Eijsink, V.G.H. (2010) An oxida- tive enzyme boosting the enzymatic conversion of recalci- trant polysaccharides. *Science* 330: 219–222.
Wang, K., Mao, H., and Li, X. (2018) Functional characteris- tics and influence factors of microbial community in sew- age sludge composting with inorganic bulking agent. *Bioresour Technol* 249: 527–535.
Wi،sniewski, J.R., Zougman, A., Nagaraj, N., and Mann, M. (2009) Universal sample preparation method for proteome analysis. *Nat Meth* 6: 359–362.
Zhang, Q., Miao, R., Liu, T., Huang, Z., Peng, W., Gan, B., *et al*. (2019) Biochemical characterization of a key laccase-like multicopper oxidase of artificially cultivable *Morchella importuna* provides insights into plant-litter decomposition. *3 Biotech* 9: e171.
Zhu, N., Liu, J., Yang, J., Lin, Y., Yang, Y., Ji, L., *et al*. (2016) Comparative analysis of the secretomes of *Schizophyllum commune* and other wood-decay basidio- mycetes during solid-state fermentation reveals its unique lignocellulose-degrading enzyme system. *Bio- technol Biofuels* 9: 42.

Supporting Information

Additional Supporting Information may be found in the online version of this article at the publisher's web-site:

Appendix S1: Supporting information

Fig. S1. Pairwise synteny of scaffolds between the genomes of *M. importuna* strains SCYDJ1-A1 (X-axis) and CCBAS932 (Y-axis). The VISTA program (Martin *et al*., 2004) integrated in the JGI Annotation Pipeline was used for pairwise align- ment of scaffolds as well as visualization of the alignment results. Threshold of sequence length with continuous high homology was set at 50 bp cut-off. The dot-plot figure was extracted from the JGI MycoCosm genome portal of *M. importuna* SCYDJ1-A1.

Fig. S2. ENB temperature measured by electronic thermom- eter sensors inserted into three testing ENBs. Values are mean of three replicates.

Fig. S3. Time-course changes in the content of organic com- pounds and mineral elements in fruiting bodies. The

coloured columns indicate mean of three biological repli- cates, with standard deviations. Significance of difference was judged by one-way ANOVA. A full list of all *p*-values is provided in Table S8.

Fig. S4. Enrichment of ^{15}N in ENB which were placed on the mushroom bed of a ^{15}N-labeled soil, indicating that decom- position of ENB by *M. importuna* led to assimilation of N from soil towards ENB, during the first 15 days. Significant difference between day 0 and day 15 was judged by *t* test. Samples with a significantly increased level of ^{15}N relative abundance are labeled with asterisks. The *p*-values are pro- vided in Table S8.

Fig. S5. All the 88 CAZy-proteins of *M. importuna* SCYDJ1-A1 identified in ENB. Expression levels of the transcripts and pro- teins were estimated by RNA-Seq and nanoLC-MS/MS, respectively. Steady-state transcript level (in RPKM) and pro- tein relative abundance are mean of three biological replicates. ND: not detected. Functions of the CAZymes were predicted according to their nearest analogs whose activities had been characterized in previous studies, as provided by the CAZy database. Significant up- or down-regulation was judged by fold-change > 2 or fold-change < 0.5, respectively, while FDR- corrected *p*-value < 0.05. Fold-change values and *p*-values are provided in Table S8.

Fig. S6. Counts of proteins showing significant up-regulation (fold-change > 2 and *p*-value < 0.05), significant down- regulation (fold-change > 0.5 and *p*-value < 0.05) or no signifi- cant shift, during days 15-45 or during days 45-75, respectively. Proteins of the metaproteomes of the major fungal taxa in ENB (*M. importuna* SCYDJ1-A1, *Mortierella*, *Trichoderma*, *Mono-dictys*, *Peziza*, *Cladosporium*, *Neonectria*, *Penicillium*, *Fusar- ium*, *Oliveonia*, *Plectosphaerella*), or those belonging to
M. importuna SCYDJ1-A1 only, were counted respectively. Subset panels show expressing regulation in the CAZymes of
M. importuna SCYDJ1-A1. Areas of the circular sectors are all proportional to gene counts.

Fig. S7. A. Distribution of occurrence of genes coding for CAZymes involved in decomposition of plant polysaccharides, lignin and lipids, compared between the genomes of the com- mercially cultivated mushrooms *M. importuna* SCYDJ1-A1,
A. bisporus, *P. ostreatus* and *L. edodes*. B. Presence of CAZymes in the proteomic profiles of *M. importuna* SCYDJ1-A1,
P. ostreatus and *A. bisporus*. The CAZy-genes are sorted in cat- egories according to their targeted substrates. Significant over- representation and under-representation were judged by Fish- er's exact test shown in Table S7. The number of expressed CAZy-proteins of *P. ostreatus* and *A. bisporus* are calculated from available previous studies (Patyshakuliyeva *et al*., 2015; Fernández-Fueyo *et al*., 2016), while *M. importuna* SCYDJ1-A1 is from this study.

Fig. S8. Rarefaction curves of bacterial 16S (a) and fungal ITS (b) sequences. ENB at day 15, 45 and 75 are shown by *solid lines*, *dash lines* and *dot lines*, respectively. The three repli- cates of each time-point are coloured in *red*, *green* and *blue*.

Table S1. Genome completeness and assembly metrics of *M. importuna* SCYDJ1-A1 and CCBAS932 strains.

Table S2. Comparison of gene-model characteristics between *M. importuna* SCYDJ1-A1 (*red*) and CCBAS932 (*blue*) strains.

Table S3. 9783 common genes shared by the SCYDJ1-A1 and CCBAS932 strains of *M. importuna*, determined by BlastP Best Reciprocal Hit analysis. The table is of big size, and is therefore provided as an individual Excel file available online: TableS3.xls.

Table S4. Initial state of physiochemical characteristics of the pre-homogenized soil used as the mushroom bed for morel cultivation.

Table S5. Content of chemicals in ENB at day 0, 15, 45 and 75.

Table S6. Proteins identified in the metaproteomes, with relative abundance of the three replicates at day 15, 45 and 75. The table is of big size, and is therefore provided as multiple working-sheets in an individual Excel file available online: TableS6.xls.

Table S7. Crosstabs showing all the results of Fisher's exact test conducted in this study. Significant over- representation is judged by adjusted residual value
> 1.96 (upper limit of 95% confidence of +1), and signifi- cant under-representation by adjusted residual value <
−1.96 (lower limit of 95% confidence of −1), as the criteria proposed by MacDonald and Gardner (2000). The table is of big size, and is therefore provided as multiple working-sheets in an individual Excel file available online: TableS7.xls.

Table S8. *p*-values of all the statistical comparisons (except for Fisher's exact test) in this study. The table is of big size, and is therefore provided as multiple working-sheets in an individual Excel file available online: TableS8.xls.

Table S9. Methods for enzymatic activity estimation.

Table S10. User-defined reference metagenome.

Table S11. Mapping rate of RNA-Seq reads.